ACS APPLIED MATERIALS & INTERFACES

Research Article

www.acsami.org

Rare-Metal-Free Flexible Counter Electrodes for Dye-Sensitized Solar-Cells Produced Using Wet Processes Only

Issei Okada and Seimei Shiratori*

School of Integrated Design Engineering, Keio University, 3-14-1 Hiyoshi, Kohoku-ku, Yokohama, Kanagawa 223-8522, Japan

ABSTRACT: Dye-sensitized solar-cells (DSCs) are cheap because they are produced using low-cost materials and simple manufacturing processes. However, the substrates of DSC counter electrodes are sputtered with a transparent conductive oxide and platinum. This involves vacuum manufacturing processes and high-cost (rare-metal) materials, and increases the costs of DSCs. In this study, we used non-rare-metal low-cost materials and simple wet processes, using combined poly(3,4-ethylenedioxythiophene)/poly(styrenesulfonate) (PEDOT/PSS) and Ag network (Ag NW) substrates. To solve the problem of Ag NW corrosion by the iodine electrolyte, we hot-pressed the Ag NW substrate and covered with a PEDOT/PSS layer as a barrier against iodine. The PEDOT/PSS layer acted as a catalyst and cells using an Ag NW covered with PEDOT/PSS generated electricity with illumination from both sides. The cell performance was improved by using a PEDOT/PSS layer containing 20 wt % TiO_2 nanoparticles (NPs). The performance of the DSSC cell with an Ag NW substrate covered with a PEDOT/PSS layer containing TiO_2 NPs (5.13%) was higher than that of a cell using an indium tin oxide substrate covered with the same layer (4.91%). These values are very similar to those of cells using a platinum counter electrode (5.36%). This research showed the possibility of replacing conventional high-cost counter electrodes with low-cost materials, and using only simple wet processes.

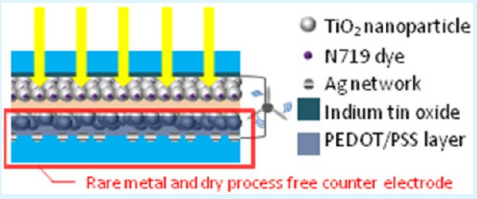

KEYWORDS: *dye-sensitized solar-cells, counter electrodes, PEDOT/PSS, TiO_2, Ag, wet process*

1. INTRODUCTION

Dye-sensitized solar-cells (DSCs) have attracted interest as substitutes for conventional silicon solar-cells because of their low-cost materials and easy fabrication processes.[1,2] Furthermore, flexible DSCs can be obtained using plastic substrates and low-temperature fabrication (less than 150 °C). This enables roll-to-roll processes to be used, and lowers the fabrication costs.[3−6] DSCs are therefore potentially low-cost solar-cells. However, the counter electrodes of DSCs are generally fabricated using transparent conductive oxide (TCO) substrates sputtered with platinum, so their production involves rare metals and vacuum processes,[7] i.e., fabrication of the counter electrodes involves high-cost materials and processes. In DSCs, the counter electrodes work as catalysts for reducing I_3^- to I^- in the electrolyte.[8] The counter electrodes therefore have an important role in generating electricity efficiently, and platinum is generally used as the counter electrode because of its high catalytic activity.[7] Recently, alternative materials and processes have been reported. The candidates for alternative materials are generally conductive polymers, for example, polypyrrole, polyaniline, and poly(3,4-ethylenedioxythiophene) (PEDOT), which have relatively high conductivities, high catalytic activities, and high stabilities.[9] Poly(4-styrenesulfonic acid) (PSS)-doped PEDOT (PEDOT/PSS) is more robust against reduction of I_3^- to I^- in redox reactions on DSC counter electrodes, and the PEDOT/PSS layer is fabricated by wet process coating. PEDOT/PSS is one of the best candidates for an alternative material to platinum. However, counter electrodes fabricated with a PEDOT/PSS layer have a low fill factor (FF) because the layer has a smooth surface, and therefore a small surface area.[10−12] Solutions to this problem have been reported. Miyasaka et al. reported that a PEDOT/PSS layer containing TiO_2 nanoparticles (NPs) and indium tin oxide (ITO) has a high surface area and a high FF.[13,14] Counter electrodes with PEDOT/PSS layers containing semiconductive or conductive NPs have also been reported and the cell performances were similar to those of DSCs with platinum counter electrodes.[15−17] There are many reports of alternative materials and processes, but few of them describe low-cost counter electrodes without a TCO substrate. In general, the TCO substrates used for counter electrodes are fluorine-doped tin oxide and ITO substrates.[7,13,14] TCO substrates are fabricated using vacuum processes and high-cost materials. It is therefore desirable to replace TCO substrates with substrates produced using low-cost materials and processes. To the best of our knowledge, there are no reports of counter electrodes fabricated using only wet coating processes and non-rare-metal materials.

In this research, counter electrodes were fabricated using wet coating processes and nonrare-metal materials, with PEDOT/PSS and Ag network (Ag NW) substrates. The PEDOT/PSS layers and Ag NW substrates were fabricated using a doctor-blade method, which is a wet coating process. The produced counter electrodes are transparent, and are flexible because they

Received: January 8, 2013
Accepted: April 9, 2013
Published: April 9, 2013

 © 2013 American Chemical Society dx.doi.org/10.1021/am4000722 | ACS Appl. Mater. Interfaces 2013, 5, 4144−4149

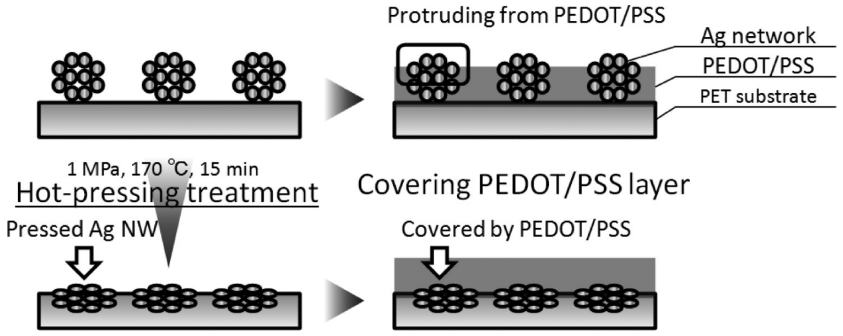

Figure 1. Scheme for incorporating Ag NW into PEDOT/PSS layer using hot-pressing treatment.

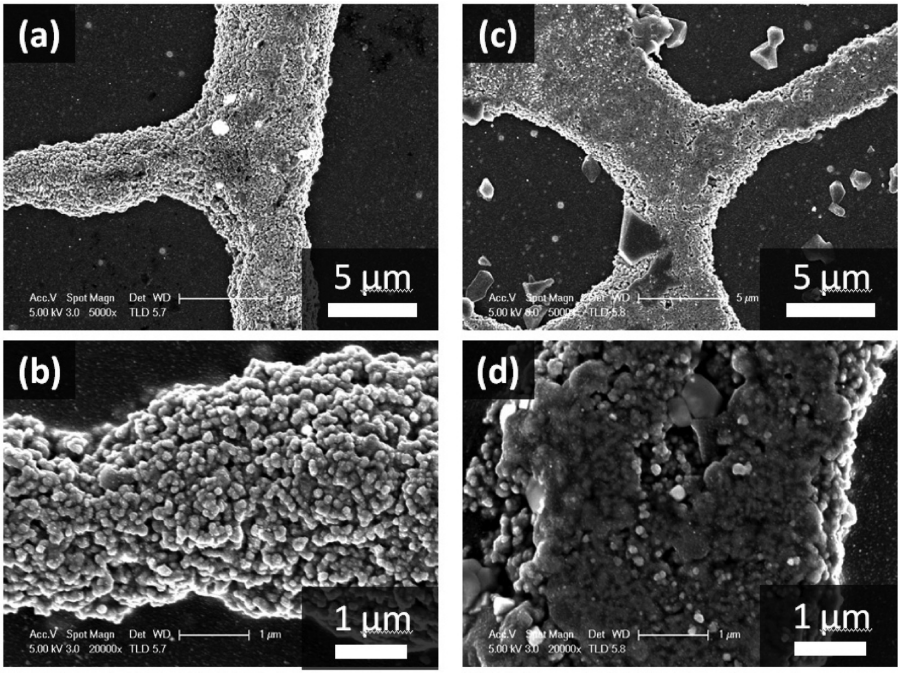

Figure 2. FE-SEM images of (a, b) untreated Ag NW (nonpre-Ag NW), and (c, d) hot-pressed Ag NW (press-Ag NW).

are fabricated at low temperature (80 °C). DSCs with transparent counter electrodes are able to generate electricity from both sides. The addition of a PEDOT/PSS layer mixed with TiO_2 NPs on the pure PEDOT/PSS layer significantly improved the cell performance.

2. EXPERIMENTAL SECTION

2.1. Fabrication Process for Ag NW Substrates. Ag NW were fabricated on polyethylene terephthalate by spreading a paste containing Ag NPs, pure water, toluene, and surfactants. An Ag NW was formed as follows. First, phase separation between water and toluene occurred, and the Ag NPs were surrounded by water drops. The water and toluene then evaporated and the Ag NW was formed. This fabrication technique and the Ag NW substrates were provided by the Toda Industrial Corporation.[18]

2.2. Hot-Pressing Treatment of Ag NW Substrates. The fabricated Ag NW substrates were pressed with heating at 170 °C and a pressure of 1 MPa for 15 min (press-Ag NW). This treatment was performed using hot-pressing equipment, and the Ag NW substrates were sandwiched between two silicon rubber sheets and two glass substrates, with the silicon rubber sheets on the outside and glass substrates on the inside. The silicon rubber sheets and glass substrates enable the Ag NW substrate to be pressed with an equal pressure and smooth surface, respectively.

2.3. Preparation of Catalytic Part of Counter Electrode. The catalytic part of the counter electrode was fabricated on the press-Ag NW substrate. The press-Ag NW substrate was hydrophilized using a plasma treatment. The treated press-Ag NW substrates were covered with PEDOT/PSS (Orgacon S305, Afga, Mortsel, Germany) by a squeegee method; the PEDOT/PSS acts as a catalyst and a barrier layer against the iodine electrolyte. The press-Ag NW substrate covered with PEDOT/PSS (PEpress-Ag NW) was heated on a hot plate in air at 80 °C for 15 min. The PEpress-Ag NW substrate was hydrophilized using a plasma treatment, and a PEDOT/PSS paste mixed with 20 wt % TiO_2 NPs was spread on the PEpress-Ag NW substrates (TPEpress-AgNW) as a layer with high catalytic activity. The paste was stirred for 24 h. These layers were heated on a hot plate in air at 80 °C for 15 min.

2.4. Preparation of TiO_2 Photoanodes. TiO_2 mesoporous films were deposited on a washed ITO glass substrate (ITO glass, Geomatec, Yokohama, Japan, 10 Ω/□) by a squeegee method using a paste containing TiO_2 NPs. The deposited TiO_2 films were sintered at 150 °C for 15 min and then immersed in a dye solution at 60 °C for 24 h. The dye solution was a 0.3 mM anhydrous ethanol solution of *cis*-bis(isothiocyanato)-bis(2,20-bipyridyl-4,40-icarboxylato)-ruthenium(II) bis(tetrabutylammonium) (N719, Solaronix, Aubonne, Switzerland). The dye-adsorbed TiO_2 films were removed from the dye solution and rinsed with ethanol. The dye-absorbed TiO_2 films on the ITO glass substrate were used as TiO_2 photoanodes.

dx.doi.org/10.1021/am4000722 | ACS Appl. Mater. Interfaces 2013, 5, 4144−4149

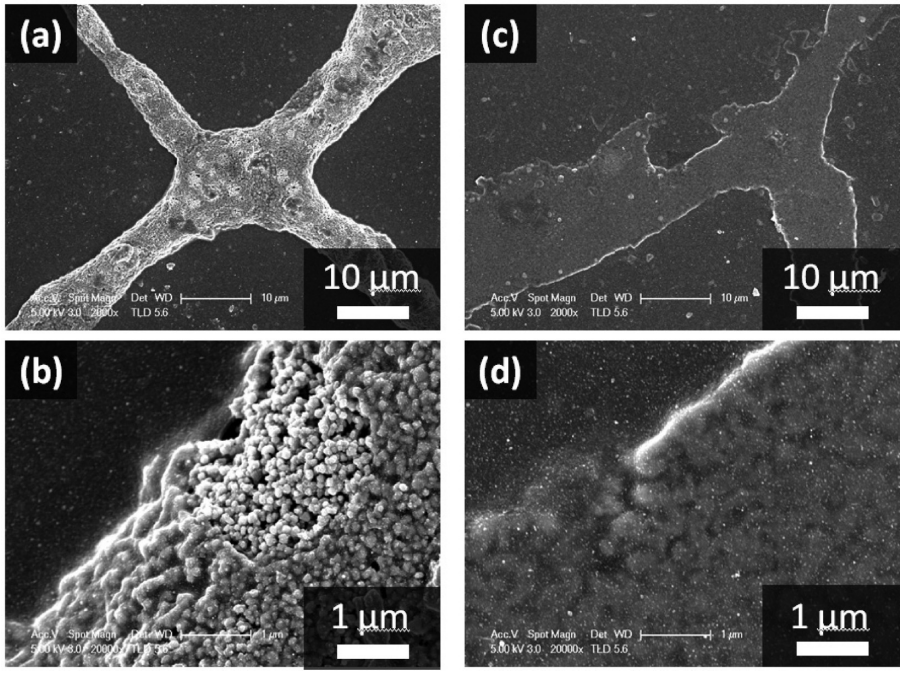

Figure 3. FE-SEM images of (a, b) nonpre-Ag NW, and (c, d) press-Ag NW, which are all covered with PEDOT/PSS layer.

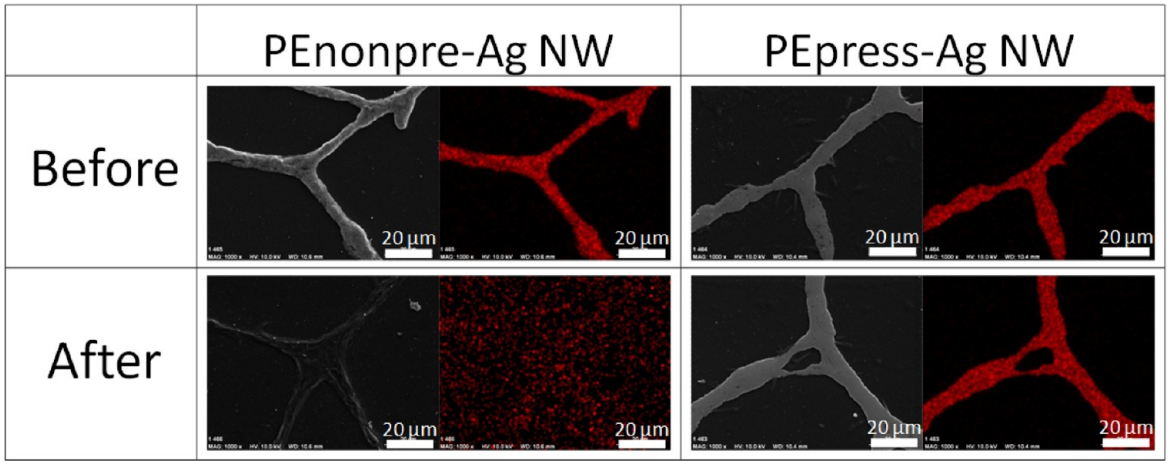

Figure 4. FE-SEM images (gray) and EDX images (red and black) of NWs before and after durability tests against iodine electrolyte: left, PEnonpre-Ag NW; right, PEpress-Ag NW.

2.5. DSSC Assembly. The obtained TiO_2 photoanodes and counter electrode were sandwiched between spacer films, with a small quantity of electrolyte solution between the electrodes. The electrolyte solutions consisted of 0.1 M LiI, 0.05 M I_2, 0.6 M 1-propyl-2,3-dimethylimidazolium iodide (DMPII, Solaronix), and 0.5 M *tert*-butylpyridine (Aldrich, St Louis, MO, USA) in acetonitrile solvent.

2.6. Characterization Measurements. The surface morphologies were investigated using field-emission scanning electron microscopy (FE-SEM; S-4700, Hitachi Ltd., Tokyo, Japan). The Ag NW heights were determined using a laser microscope (VK-9700 Generation II, KEYENCE, Osaka, Japan). Sheet resistances were measured using the four-point probe method (Model 236 source measuring unit, Keithley, Japan). Durability tests against the iodine electrolyte were performed as follows. First, PEn-Ag NW and PEp-Ag NW substrates were soaked in the iodine electrolyte for a week. They were then removed from the iodine electrolyte and their sheet resistances were measured using the four-point probe method, and they were examined using energy-dispersive X-ray spectroscopy (EDX). These measurements and examinations were also carried out on the PEn-Ag NW and PEp-Ag NW substrates before the durability tests. The transmittance of each substrate was measured using ultraviolet−visible (UV−vis) absorption spectroscopy (Shimadzu, Japan). The photocurrent density−voltage curves of the cells were measured under illumination with an AM 1.5 solar simulator (100 mW cm^{-2}) with a device and mask area of 0.2827 cm^2. A 500-W Xe lamp (UXL-500SX, Ushio Inc., Tokyo, Japan) was used as the light source.

3. RESULTS AND DISCUSSION

3.1. Durability of Ag NW against Iodine Electrolyte. Ag NW substrates have the problem that Ag NW is corroded by the iodine electrolyte. To prevent corrosion of the Ag NW by the iodine electrolyte, the Ag NW substrates were pressed with heating at 170 °C, and then covered with a PEDOT/PSS layer. Figure 1 shows the scheme for preventing Ag NW corrosion by the iodine electrolyte. The PEDOT/PSS layer isolates the Ag NW from the iodine electrolyte because the PEDOT/PSS layer is inert to iodine. However, the untreated Ag NW (non-pre-Ag NW) was not perfectly covered with PEDOT/PSS. The

PEDOT/PSS layer at the Ag NW was thinner or broken because the PEDOT/PSS layer is flat and the Ag NW has a height of 2.91 μm. In contrast, the hot-pressed Ag NW (press-Ag NW) is perfectly covered by the PEDOT/PSS layer. The PEDOT/PSS layer was not thinner or broken at the Ag NW because the height of the Ag NW was reduced by the hot-pressing treatment. This is why the Ag NW substrates were hot-pressed. Figure 2 shows SEM images of the Ag NW substrates before and after the hot-pressing treatment. A comparison of images a and c in Figure 2 shows that parts of the hot-pressed Ag NW were flattened and it was difficult to observe each Ag NP. A comparison of images b and d in Figure 2 shows that the Ag NPs were well-combined after the hot-pressing treatment. This is why it was difficult to observe Ag NPs. Furthermore, the height of the Ag NW was lowered from 2.91 to 0.35 μm, as measured by laser microscopy. Figure 3 show SEM images of the Ag NW covered with PEDOT/PSS (PE-Ag NW). Figure 3c shows that the Ag NW without hot-pressing protruded from the PEDOT/PSS layer and was not perfectly covered by the PEDOT/PSS layer, whereas Figure 3d shows that the press-Ag NW was perfectly covered by the PEDOT/PSS layer. These results are consistent with the scheme in Figure 1, and are attributed to the Ag NW height. The durabilities against the iodine electrolyte of the non-pre-Ag NW and press-Ag NW substrates covered with PEDOT/PSS (PEnonpre-Ag NW and PEpress-Ag NW, respectively) were examined. Figure 4 shows the SEM images and EDX images before and after the durability tests against the iodine electrolyte. In the EDX images, the red particles represent Ag. After the durability tests, the PEnonpre-Ag NW substrate lost the Ag NW. This result is attributed to the experimental finding that the Ag NW was imperfectly covered by the PEDOT/PSS layer, as shown in Figure 3b. In contrast, the PEpress-Ag NW substrate retained the Ag NW even after the durability tests. This result showed that durability against the iodine electrolyte was achieved and this is attributed to the fact that the Ag NW was perfectly covered by the PEDOT/PSS layer, as shown in Figure 3d. The presence of the Ag NW was also examined by measuring the sheet resistances of the substrates. The sheet resistance of the PEnonpre-Ag NW substrate increased from 12.6 Ω/□ to 167 Ω/□ after the durability tests. The sheet resistance value of 167 Ω/□ was similar to that of the PEDOT/PSS layer without the Ag NW, whereas the PEpress-Ag NW substrate had similar sheet resistances before and after the durability tests, i.e., 4.91 Ω/□. These results are consistent with the EDX images in Figure 4, and the durability tests proved that the PEpress-Ag NW substrates have durability against the iodine electrolyte.

3.2. Comparison of ITO Substrates and Ag NW Substrates. In this study, Ag NW substrates were used as substitutes for ITO glass substrates. ITO substrates have low resistances and high transmittances in the visible range. Figure 5 shows a comparison of the sheet resistances of ITO and Ag NW substrates. The sheet resistance of the Ag NW substrate was reduced by hot-pressing treatment. The sheet resistance of the press-Ag NW substrate changed little because it was covered by a PEDOT/PSS layer. A comparison of the sheet resistances of the press-Ag NW and ITO substrates shows that the sheet resistance of the press-Ag NW substrate was much lower than that of the ITO substrate. (The TPEpress-Ag NW substrate had a sheet resistance of 10.1 Ω/□.) This result shows that, in terms of sheet resistance, the press-Ag NW substrates are more suitable for DSCs than the ITO substrates

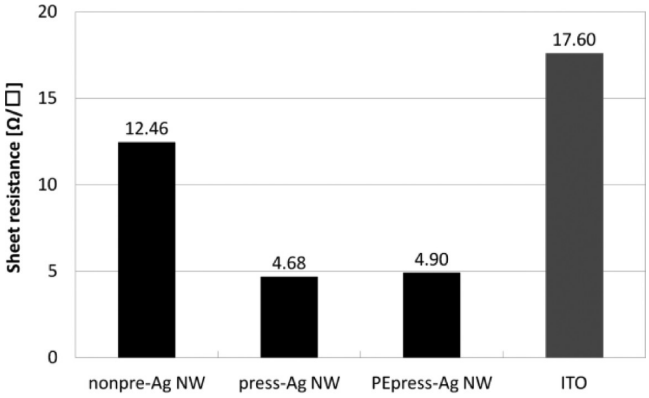

Figure 5. Sheet resistances of nonpre-Ag NW, pre-Ag NW, PEpre-Ag NW, and ITO substrates.

are. Moreover, Ag NW substrates are superior to ITO substrates in terms of manufacturing processes because Ag NW substrates can be fabricated using nonrare-metal materials and simple wet processes; in contrast, ITO substrates are fabricated using a rare metal (indium) and vacuum processes. Figure 6 shows a comparison of the transmittances of the ITO

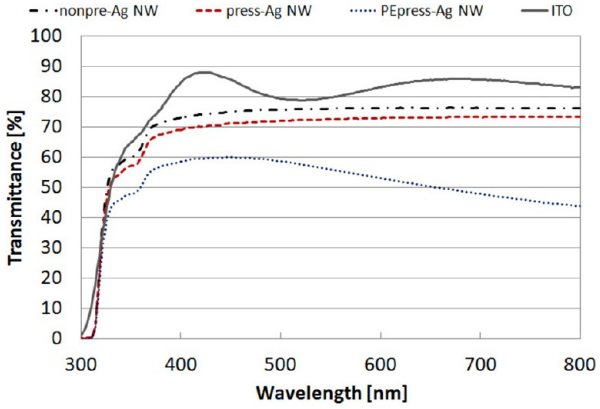

Figure 6. Transmittances of non-pre-Ag NW, press-Ag NW, PEpress-Ag NW, and ITO substrates.

and Ag NW substrates. In terms of transmittance, the ITO substrates were superior to all the Ag NW substrates. The transmittance of the non-pre-Ag NW substrate was little changed by hot-pressing treatment and the value decreased to approximately 60% of the original transmittance on covering with a PEDOT/PSS layer. However, this 60% transparency is sufficient for using these PEpress-Ag NW substrates as counter electrodes for see-through or both-sides-generation DSCs. (The TPEpress-Ag NW substrates had no transmittance.)

3.3. Cell Performances of DSCs with PEpress-Ag NW Counter Electrodes. The above results show that PEpress-Ag NW substrates have durability against iodine electrolytes and could be used instead of ITO substrates. We therefore used PEpress-Ag NW substrates as counter electrodes in DSCs.

Figure 7 shows the photocurrent density−voltage curves of cells using PEpress-Ag NW counter electrodes. In Figure 7, the solid and dotted lines represent the J−V curves for front illumination and rear illumination, respectively. The front and rear illuminations are the illuminations from the anode side and the counter electrode side, respectively. In general, light is taken into cells from the anode side (front illumination) and is not

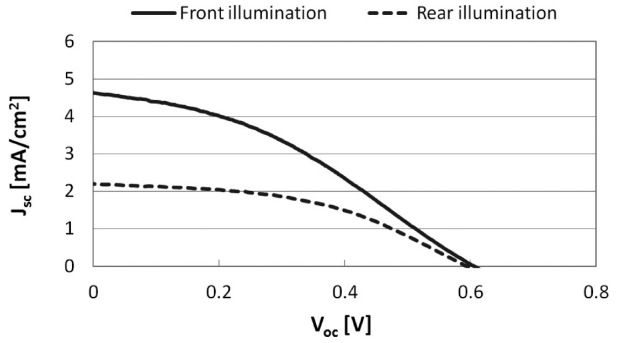

Figure 7. Photocurrent density (J_{sc})−voltage curves for cells using PEpress-Ag NW counter electrodes with front (solid line) and rear (dot line) illumination.

able to enter from the counter electrode side (rear illumination) because conventional platinum layers have no transparency. However, PEpress-Ag NW counter electrodes have approximately 60% transmittance at 450 nm. PEp-Ag NW counter electrodes therefore allow light to enter the cells. Figure 7 and Table 1 show the cell performance of cells using

Table 1. Photovoltaic Performances of Cells Fabricated with PEpress-Ag NW Counter Electrodes, with Illumination from Front or Rear Side

illumination side	J_{sc} (mA/cm^2)	V_{oc} (V)	FF	efficiency (%)
front	4.63	0.61	0.36	1.02
rear	2.21	0.59	0.46	0.61

PEpress-Ag NW counter electrodes with front and rear illumination. The conversion efficiencies were 1.02% and 0.61% for front and rear illumination, respectively. The cells with rear illumination had lower conversion efficiencies than those with front illumination did. This is attributed to the transmittance of the PEpress-Ag NW counter electrode, which is 60%; in other words, the PEpress-Ag NW counter electrodes cuts out 40% of the light that should enter the cell. This is proved by the lower photocurrent densities (Jsc) of cells with rear illumination. As a result, the cells with rear illumination had lower cell performances, although electron generation was shown by the illuminations at both sides. These cell performances were comparatively low because the PEDOT/PSS layer had a low catalytic activity as a result of its smooth surface morphology, shown in Figure 3. The cell performances were improved by adding a layer of PEDOT/PSS mixed with TiO_2 NPs on the PEpress-Ag NW (TPEpress-Ag NW) counter electrodes; this layer has high porosity and a high surface area. These results are discussed in the next section.

3.4. Improvement of Cell Performance by PEDOT/PSS Mixed TiO_2 NPs Layer. Figure 8 shows the surface of the TPEpress-Ag NW counter electrode, which has high porosity and a high surface area. This high surface area leads to high catalytic activity and high cell performance. Figure 9 shows the $J-V$ curves and Table 2 shows the photocurrent densities (J_{sc}), open-circuit voltages (V_{oc}), FFs, and conversion efficiencies of cells with platinum counter electrodes, TPEpress-Ag NW counter electrodes, and TPE-ITO counter electrodes. The TPE-ITO counter electrode is an ITO substrate covered with PEDOT/PSS mixed with 20 wt % TiO_2 NPs. A comparison of the PEpress-Ag NW and TPEpress-Ag NW counter electrodes showed that the performance of the cell with the PEpress-Ag

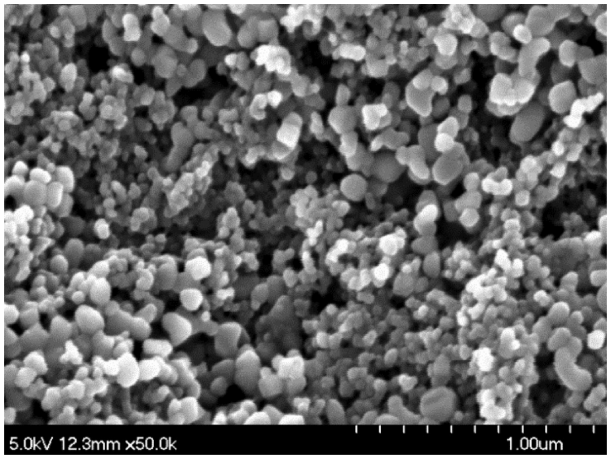

Figure 8. FE-SEM image of surface morphology of TPEpress-Ag NW counter electrode.

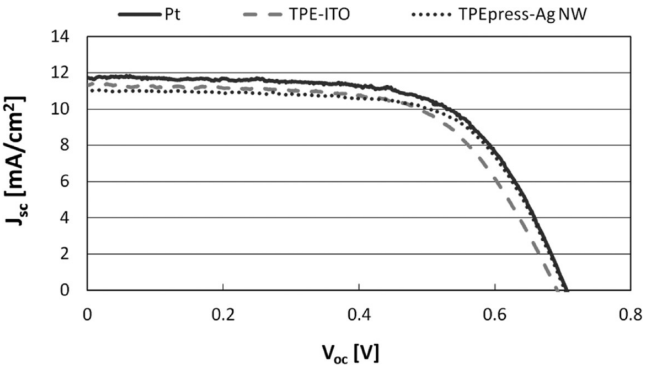

Figure 9. Photocurrent density (J_{sc})−voltage curves for cells using platinum counter electrode, TPE-ITO counter electrode, and TPEpress-Ag NW counter electrode.

Table 2. Photovoltaic Performance of Cells Fabricated with Platinum, TPEpress-Ag NW, and TPE-ITO Counter Electrodes

counter electrode	J_{sc} (ma/cm^2)	V_{oc} (V)	FF	efficiency (%)
Pt	11.71	0.71	0.65	5.36
TPEpress-Ag NW	11.01	0.71	0.66	5.13
TPE-ITO	11.34	0.69	0.63	4.91

NW counter electrode was improved from 1.02% to 5.13% by adding a PEDOT/PSS layer containing TiO_2 NPs. This significant improvement in the cell performance is attributed to the high surface area of the TPEpress-Ag NW counter electrode. This is consistent with the improvement in the FF value. In a comparison of the TPEpress-Ag NW and TPE-ITO counter electrodes, the conversion efficiency of the cell with the TPEpress-Ag NW counter electrode was higher than that of the cell with a TPE-ITO counter electrode. This result is attributed to the slightly higher FF of the cell with the TPEpress-Ag NW counter electrode, and this higher FF is consistent with the lower sheet resistance of the press-Ag NW substrate compared with that of the ITO substrate. This result showed the possibility of replacing ITO substrates. In a comparison of TPEpress-Ag NW and conventional platinum counter electrodes, the cell with an TPEpress-Ag NW counter electrode had a cell performance very similar to that of the cell with a platinum counter electrode. The TPEpress-Ag NW counter electrode

could therefore be used instead of conventional platinum counter electrodes. These two comparisons confirmed the possibility of replacing conventional ITO substrates sputtered with platinum as counter electrodes. TPEpress-Ag NW counter electrodes are also superior to conventional platinum counter electrodes in terms of cost and environmental burden because the TPEpress-Ag NW counter electrodes were fabricated using low-cost nonrare-metal materials and simple wet manufacturing processes.

4. CONCLUSIONS

Hot-pressing decreased the height of an Ag NW; corrosion of the Ag NW by an iodine electrolyte was prevented by covering the Ag NW with a PEDOT/PSS layer. The sheet resistance of the Ag NW decreased as a result of hot-pressing, and was much lower than those of ITO substrates. Cells using this counter electrode showed electron generation at both sides on illumination. The cell performances were 1.02% and 0.61% for front and rear illumination, respectively. This cell performance was significantly improved by adding a layer of PEDOT/PSS mixed with TiO_2 NPs on a pure PEDOT/PSS layer; the cell performance was 5.13%. As a result of this significant improvement, the cell performance became higher than that of a cell using an ITO substrate covered with the same layer as the counter electrode, and the performance was almost the same as those of cells using platinum counter electrodes. This study showed the possibility of replacing platinum counter electrodes by counter electrodes fabricated using low-cost, nonrare-metal materials and simple wet manufacturing processes.

AUTHOR INFORMATION

Corresponding Author

*E-mail: shiratori@appi.keio.ac.jp.

Notes

The authors declare no competing financial interest.

ACKNOWLEDGMENTS

We thank the Toda Industrial Corporation for supplying the Ag NW substrates.

REFERENCES

(1) O'Regan, B.; Gratzel, M. *Nature* **1991**, *353*, 737−740.
(2) Barbe, C. J.; Arendse, F.; Comte, P.; Jirousek, M.; Lenzmann, F.; Shklover, V.; Gratzel, M. *J. Am. Ceram. Soc.* **1997**, *71*, 3157−3171.
(3) Kijitori, Y.; Ikegami, M.; Miyasaka, T. *Chem. Lett.* **2007**, *36*, 190−191.
(4) Miyasaka, T.; Ikegami, M.; Kijitori, Y. *J. Electrochem. Soc.* **2007**, *154*, A455−A461.
(5) Yamaguchi, T.; Tobe, N.; Matsumoto, D.; Arakawa, H. *Chem. Commun.* **2007**, 4767−4769.
(6) Miyasaka, T. *J. Phys. Chem. Lett.* **2011**, *2*, 263−269.
(7) Fang, X.; Ma, T.; Guan, G.; Akiyama, M.; Abe, E. *J. Photochem. Photobiol., A* **2004**, *164*, 179−182.
(8) Papageorgiou, N.; Maier, W. F.; Graztel, M. *J. Electrochem. Soc.* **1997**, *144*, 876−884.
(9) Bay, L.; West, K.; Winther-Jensen, B.; Jacobsen, T. *Sol. Energy Mater. Sol. Cells* **2006**, *90*, 341−351.
(10) Saito, Y.; Kitamura, T.; Wada, Y.; Yanagida, S. *Chem. Lett.* **2002**, *31*, 1060−1061.
(11) Shibata, Y.; Kato, T.; Kado, T.; Shiratuchi, R.; Takashima, W.; Kaneto, K.; Hayase, S. *Chem. Commun.* **2003**, 2730−2731.
(12) Xia, J.; Masaki, N.; Jiang, K.; Yanagida, S. *J. Mater. Chem.* **2007**, *17*, 2845−2850.
(13) Muto, T.; Ikegami, M.; Kobayashi, K.; Miyasaka, T. *Chem. Lett.* **2007**, *36*, 804−805.
(14) Muto, T.; Ikegami, M.; Miyasaka, T. *J. Electrochem. Soc.* **2010**, *157*, B1195−B1200.
(15) Xu, H.; Zhang, X.; Zhang, C.; Liu, Z.; Zhou, X.; Pang, S.; Chen, X.; Dong, S.; Zhang, Z.; Zhang, L.; Han, P.; Wang, X.; Cui, G. *ACS Appl. Mater. Interfaces* **2012**, *4*, 1087−1092.
(16) Yue, G.; Wu, J.; Xiao, Y.; Lin, J.; Huang, M. *Electrochim. Acta* **2012**, *67*, 113−118.
(17) Kitamura, K.; Shiratori, S. *Nanotechnology* **2011**, *22*, 195703.
(18) Garbar, A.; De La Vega, F.; Matzner, E.; Sokolinsky, C.; Rosenband, V.; Kiselev, A.; Lekhtman, D. U.S. Patent 7 736 693, June 15, 2010.